

OXYGEN SENSING BEHAVIOUR OF Pr DOPED $\text{Eu}_{1-x}\text{Pr}_x\text{Ba}_2\text{Cu}_3\text{O}_{7-\delta}$ CERAMIC RODS WITH HOT-SPOT

M. I. Adzam, M. I. M. Yusof and A. K. Yahya

Faculty of Applied Sciences Universiti
Teknologi MARA
40450 Shah Alam, Selangor Malaysia e-mail:
mohdi113@salam.uitm.edu.my

Abstract

In this study, $\text{Eu}_{1-x}\text{Pr}_x\text{Ba}_2\text{Cu}_3\text{O}_{7-\delta}$ ($x = 0.0, 0.05, 0.10$, and $x = 0.20$) ceramic rectangular rods were prepared by the solid-state reaction method to investigate the effect of Pr doping on oxygen sensing behaviours. X-ray powder diffraction analysis showed all rods were orthorhombic in structure with reduction in orthorhombicity upon doping. For all samples, the I - V curve showed a relatively constant output current after the appearance of hot-spot. The magnitude of the constant output current was observed to be decreasing with increasing Pr doping which indicates possible reduction in intrinsic hole concentration. In addition, the output current for rods with $x = 0.0, 0.05$ and 0.10 showed a sudden drop upon the appearance of hot-spot, due to the sudden increase in hot-spot temperature, before becoming slightly constant. However, the sudden drop of output current upon appearance of hot-spot was not observed when Pr was increased to $x = 0.15$ and 0.20 but instead a stable output current was observed. Interestingly, the output current after

Received: June 12, 2014; Accepted: September 2, 2014

Keywords and phrases: powders, solid state reaction, hot-spot rods, Eu_{123} , Pr substitution, oxygen sensors.

appearance of hot-spot for all rods showed strong dependency on ambient oxygen concentration. The sensitivity for each rod, however, reduces with increasing ambient oxygen concentration. The doping seems to prevent the sensitivity from dropping to almost zero as was previously reported for $\text{Eu}(\text{Ba}_{1-y}\text{Pr}_y)_2\text{Cu}_3\text{O}_{7-\delta}$ rods due to existence of Cu-O chains in the orthorhombic structure. Pr doping (for $x = 0.10$) has also resulted in better oxygen absorption response time and better output current stability compared to other rods.

1. Introduction

Of late, a novel and simple type of oxygen sensor based on RE123 (RE = Gd, Sm) ceramics was found by Takata which exploits the hot-spot phenomenon when external voltage is applied [1]. The effect of oxygen non-stoichiometry in RE123 involving Cu-O chains was identified as the underlying factor responsible for oxygen response. The constant current, after appearance of the hot-spot, depends on oxygen partial pressure in ambient atmosphere and can be used to sense oxygen without the need of an external heater [1, 2]. Uniquely, reports have suggested that elemental substitution either at Ba-site or RE-site of the RE123 system modifies the structure and oxygen sensing behaviour as well [3-7].

Initial studies on several RE123 hot-spot based sensors showed a sudden drop in output current upon formation of hot-spot, before gradually becoming constant at higher applied voltage [1, 8-10]. A recent study by Yaacob et al. [7] on oxygen sensing behaviour properties for $\text{Eu}_{1-x}\text{Ca}_x\text{Ba}_2\text{Cu}_3\text{O}_{7-\delta}$ ceramic rods, however, showed that the output current upon appearance of a hot-spot continued to increase slightly before becoming constant. The higher Ca-doping was suggested to have caused the output current to immediately stabilize upon hot-spot visibility [7]. Interestingly, our previous work on Pr doped $\text{Eu}(\text{Ba}_{1-x}\text{Pr}_x)_2\text{Cu}_3\text{O}_{7-\delta}$ rods showed no effect of the increase or drop in output current upon the appearance of hot-spot but instead, the output current became constant immediately with increasing applied voltage [4]. This behaviour of the output

current was proposed to be related to the generated heat from joule heating matching the dissipated heat upon hot-spot visibility.

In addition, Pr doped $\text{Eu}(\text{Ba}_{1-x}\text{Pr}_x)_2\text{Cu}_3\text{O}_{7-\delta}$ also showed that the doping lowered the activation energy, E_a and resulted in faster absorption and desorption of oxygen [4]. This indicates that with increasing Pr, a faster response time, t_{res} , i.e., the time taken for the output current to reach its saturated level, is achieved for every change in the ambient oxygen concentration, pO_2 [4]. The same effect of doping on t_{res} was also observed for Ca doped $\text{Eu}_{1-x}\text{Ca}_x\text{Ba}_2\text{Cu}_3\text{O}_{7-\delta}$ rods [7]. XRD data of both studies indicated possible elemental substitution in the Eu123 system which was suggested to be the cause for the improvement of t_{res} of the output current towards change of ambient pO_2 . However, increasing Pr doping in $\text{Eu}(\text{Ba}_{1-x}\text{Pr}_x)_2\text{Cu}_3\text{O}_{7-\delta}$, has also resulted in reduction of sensitivity of output current to almost zero. Based on the lattice parameters shown in the study, structural change from orthorhombic ($x = 0$ and $x = 0.05$) to pseudo-tetragonal ($x = 0.25$) was suggested to be the factor that influenced sensitivity as the latter has much fewer Cu-O chains. This implies that the structure of the system with low Pr doping has the ability to absorb more oxygen compared to the system with high Pr doping.

On the other hand, structural studies of Pr doped $\text{Y}_{1-x}\text{Pr}_x\text{Ba}_2\text{Cu}_3\text{O}_{7-\delta}$ bulk samples revealed preservation of the orthorhombic structure even though the orthorhombicity was reduced with increasing Pr doping [12-14]. As the $\text{Y}_{1-x}\text{Pr}_x\text{Ba}_2\text{Cu}_3\text{O}_{7-\delta}$ system and the $\text{Eu}(\text{Ba}_{1-x}\text{Pr}_x)_2\text{Cu}_3\text{O}_{7-\delta}$ system are iso-structural, substitution of Pr for Eu in the $\text{Eu}_{1-x}\text{Pr}_x\text{Ba}_2\text{Cu}_3\text{O}_{7-\delta}$ system should be able to retain orthorhombic structure as well and may possibly prevent drop of sensitivity at high ambient oxygen concentration. However, this proposition has not been verified as response of output current towards ambient oxygen upon hot-spot appearance on $\text{Eu}_{1-x}\text{Pr}_x\text{Ba}_2\text{Cu}_3\text{O}_{7-\delta}$ rods and the sensitivity of the sensor rods have not, to our knowledge, been reported.

In this paper, $\text{Eu}_{1-x}\text{Pr}_x\text{Ba}_2\text{Cu}_3\text{O}_{7-\delta}$ ($x = 0, 0.05, 0.10, 0.15$ and $x = 0.2$) ceramic rods were prepared and their oxygen sensing behaviours were studied under different ambient $p\text{O}_2$ (20%-100%). The influence of orthorhombicity of the cell structure towards sensitivity of output current was analysed and discussed. In addition, repeatability and stability data of the sensing current were also presented.

2. Experimental Details

The $\text{Eu}_{1-x}\text{Pr}_x\text{Ba}_2\text{Cu}_3\text{O}_{7-\delta}$ ($x = 0, x = 0.05, x = 0.10$ and $x = 0.20$) samples were carefully synthesized by conventional solid-state reaction method. High purity (99.99%) Eu_2O_3 , BaCO_3 and Pr_6O_{11} powders were mixed and ground for 2 hours. The powder mixture was then calcined at 950°C for 24 hours in a box furnace followed by regrinding for 2 hours in an agate mortar. A second calcination was done at the same temperature and duration. The mixture was reground and pressed into pellets with diameter of 13mm and sintered at 950°C for 24 hours. The $\text{Eu}_{1-x}\text{Pr}_x\text{Ba}_2\text{Cu}_3\text{O}_{7-\delta}$ pellets were cut into several rectangular rods with dimensions of around $13\text{mm} \times 1.48\text{mm} \times 1.48\text{mm}$. Powder X-ray Diffraction (XRD) using Rigaku model D/MAX 2000 PC with Cu-K_α radiation was used to identify the sample's structure. I - V characterization of the sensor rod was conducted in a chamber at 1atm with varying $p\text{O}_2$ of 20% to 100%.

3. Results and Discussions

X-ray diffraction results indicate that all samples of $\text{Eu}_{1-x}\text{Pr}_x\text{Ba}_2\text{Cu}_3\text{O}_{7-\delta}$ were mainly single phased with minor impurity phase. Detailed analysis, as shown in Table 1 shows that all samples were of orthorhombic structure with space group $Pmmm$. Our result which indicates existence of Cu-O chains for all samples was also reported by another study [11]. While resistivity, ρ and activation energy, E_a increased with Pr doping, c -lattice parameter and unit cell volume, Ω decreased with increasing

x . Orthorhombicity of all doped samples was lower compared to undoped $x = 0$ sample. The decrease in lattice parameter, c and unit cell volume, Ω with increasing Pr doping indicates evidence of Pr substitution at Eu-site as Pr^{3+} ionic size (1.00\AA) is smaller compared to Eu^{3+} ionic size (1.07\AA). The increasing resistivity indicates that the hole concentration reduces with increasing Pr doping [4, 12].

Table 1. Lattice parameters, a , b , c , unit cell volume, Ω , resistivity, ρ (at 300K), activation energy, E_a and orthorhombicity for $\text{Eu}_{1-x}\text{Pr}_x\text{Ba}_2\text{Cu}_3\text{O}_{7-\delta}$ rods for $x = 0, 0.05, 0.10, 0.15$ and 0.20

Parameters	Pr contents (x)				
	0.0	0.05	0.10	0.15	0.20
a (nm)	0.3898	0.3909	0.3918	0.3916	0.3914
b (nm)	0.3905	0.3865	0.3872	0.3859	0.3861
c (nm)	1.1812	1.1754	1.1780	1.1744	1.1740
Ω (nm^3)	0.1798	0.1776	0.1787	0.1775	0.1774
ρ (Ω cm)	0.2070	0.2575	0.2253	0.2905	0.3731
E_a (eV)	0.0018	0.0039	0.0032	0.0233	0.0256
Orthorhombicity	0.0090	0.0057	0.0059	0.0073	0.0068

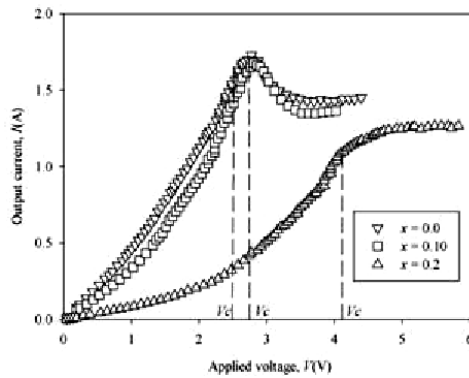
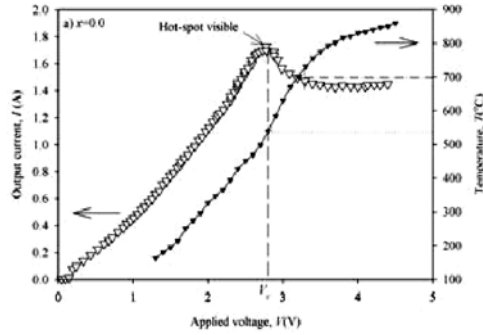


Figure 1. I - V curve measurement for $\text{Eu}_{1-x}\text{Pr}_x\text{Ba}_2\text{Cu}_3\text{O}_{7-\delta}$ ($x = 0, 0.10$, and $x = 0.20$) in ambient concentration of oxygen, $p\text{O}_2$. The dashed line indicates the hot-spot starts to be visible at applied voltage, V_c .

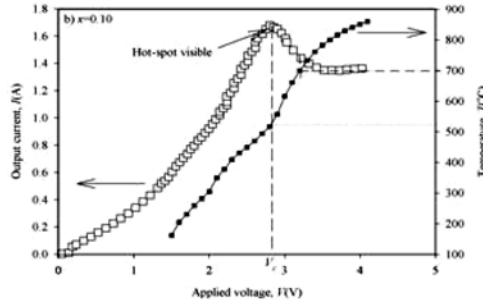
Figure 1 shows the I - V curve in ambient pO_2 for $\text{Eu}_{1-x}\text{Pr}_x\text{Ba}_2\text{Cu}_3\text{O}_{7-\delta}$ ($x = 0.0$ - 0.2) rods. By increasing the applied voltage, V the output current, I increased linearly, and when V reached a certain applied voltage, V_c a hot-spot starts to be visible. It can be clearly seen that the $x = 0.20$ rod has much higher V_c compared with other rods and a simple analysis shows that more energy was needed for the hot-spot to be visible. In addition, increasing Pr doping may have caused a reduction in mobile holes due to mixed valence Pr^{3+} and Pr^{4+} which reduces the hole concentration. Hence, a decrease in magnitude of the constant output current with increasing Pr doping was observed as can be seen in Figure 1.

Also observed in Figure 1 was the slight drop of output current upon visibility of hot-spot for $x = 0.0$ and $x = 0.10$ before becoming roughly constant with increasing applied voltage. However, for the $x = 0.20$ substitution, there was no drop of output current upon the appearance of hot-spot but instead the output current gradually increased before becoming constant. The difference in behaviour of the output currents upon hot-spot visibility as mentioned earlier can be explained based on Figure 2 where the I - V and T - V graphs for (a) $x = 0.0$, (b) $x = 0.10$ and (c) $x = 0.20$ signify the relationship between hot-spot temperature and behaviour of output current. There was a sharp increase in temperature during the formation of hot-spot for rods $x = 0.0$ (Figure 2(a)) and $x = 0.10$ (Figure 2(b)) at around $V_c = 2.8\text{V}$, but the surge in temperature was less apparent for $x = 0.20$ (Figure 2(c)) rod at around $V_c = 4.2\text{V}$. During the sharp increase in hot-spot temperature for the $x = 0.0$ and $x = 0.10$ rods, the output current dropped before becoming almost constant output current with increasing applied voltage. Interestingly, when the Pr doping was increased to $x = 0.20$, the increase in hot-spot temperature became less drastic and no drop in output current was observed. For the case of $x = 0$ and $x = 0.1$, the jump in resistivity due to drastic increase in temperature caused heat generated to be larger than heat dissipated before a balance was achieved [2]. However, for the rod with $x = 0.20$, the smaller jump in resistivity-generated heat was

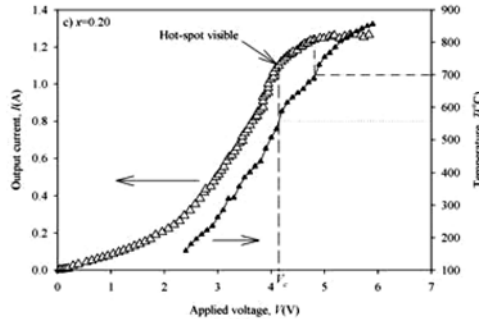
almost instantly balanced with the dissipated heat resulting in the output current swiftly becoming roughly constant upon the appearance of hot-spot.



(a)



(b)



(c)

Figure 2. I - V and T - V graphs for (a) $x = 0.0$, (b) $x = 0.10$ and (c) $x = 0.20$. The dashed line indicates V_c and the dashed-dotted line indicates the point where the temperature is at 700°C . The temperature where the hot-spot start to appear is indicated by dotted line.

The output current, I after the hot-spot also appears to exhibit pO_2 dependency [1, 3-7]. The oxygen sensing property of RE123 hot-spot can be explained in terms of absorption of ambient oxygen gas by the hot-spot before dissociating into oxide ions and holes. The overall reaction of the conduction is expressed as:



The relationship between conductivity, σ and pO_2 based on Equation (1) using the mass action law is given by:

$$\sigma \propto pO_2^{1/6}. \quad (2)$$

Equation (2) above shows the dependency of the output current on pO_2 where the slope of log of output current versus log pO_2 curve gives an ideal value of $1/6$.

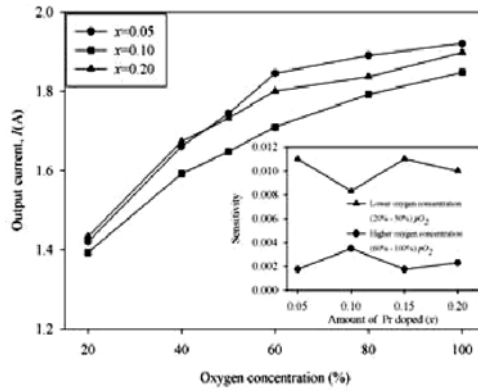


Figure 3. Current, I versus pO_2 graph for $x = 0.05$, 0.10 and $x = 0.20$. Inset shows sensitivity of output current which is defined as the response of output current towards changes of oxygen concentration upon lower and high oxygen concentration versus Pr content for 20%-50% pO_2 and 60%- 100% pO_2 respectively.

A finer analysis on the response of output current, I towards different oxygen concentrations, pO_2 is shown in Figure 3. The calculated slope from

the graph which indicates the sensitivity of output current defined as the change in output current over change in concentration oxygen is shown by inset of Figure 3. Even though the increment of the output current (sensitivity) was observed to reduce as the concentration of oxygen increases for all rods, it is worthwhile to also note that the sensitivity at lower oxygen concentration (20%-50% pO_2) is better than at higher concentration of oxygen (60%-100% pO_2). In addition, inset of Figure 3 clearly shows that there was no large variation in sensitivity upon Pr doping. The oxygen response can be explained as follows. Previous studies on substituted and un-substituted RE123 systems show that at high enough temperature, the orthorhombic structure changes to tetragonal form [14-16]. By increasing temperature, at around 400°C, the oxygen content is much reduced [17] and the number of Cu-O chains drops. In our study, the response of output current towards changes of ambient oxygen concentration was taken during constant output current where the temperature exceeded 700°C. At this temperature, oxygen was mostly driven out of the chains, and thus, many empty Cu-O chains were formed. Hence at lower ambient oxygen atmosphere, the empty Cu-O chains were able to absorb more oxygen before dissociating into oxide ions and holes. As a result, higher sensitivity of the output current was observed for each rod upon the changes of ambient oxygen from 20% to 50% pO_2 . With further increase in oxygen concentration, the absorption of ambient oxygen into the rods was less efficient due to lower availability of empty Cu-O chains and thus weakening the response of output current towards change of ambient oxygen concentration. This reduces the sensitivity of the output current when ambient oxygen was continually increased from 50% to 100% pO_2 . The reduced sensitivity at higher pO_2 for our present study is, however, an improvement when compared to our previous study of Pr substitution at Ba-site of $\text{Eu}(\text{Ba}_{1-x}\text{Pr}_x)_2\text{Cu}_3\text{O}_{7-\delta}$ rods at high ambient oxygen (40%-100% pO_2) where the sensitivity was reduced to almost zero for high Pr substitution [4]. In other words, doping of Pr at Eu-site for

$\text{Eu}_{1-x}\text{Pr}_x\text{Ba}_2\text{Cu}_3\text{O}_{7-\delta}$ rods prevented the sensitivity from dropping to nearly zero. The observation could be explained in terms of the number of Cu-O chains when Pr is substituted at Eu-site compared to Ba-site. Substitution of Pr at Ba-site transformed the orthorhombic structure of the compound to nearly tetragonal structure as well as reducing the number of Cu-O chains until none of the chains remained in the structure [4, 12, 18]. However, Pr substitution at the Eu-site preserved the orthorhombic structure. As a consequence, there were sufficient number of Cu-O chains to absorb ambient oxygen which prevented a similar drop in sensitivity.

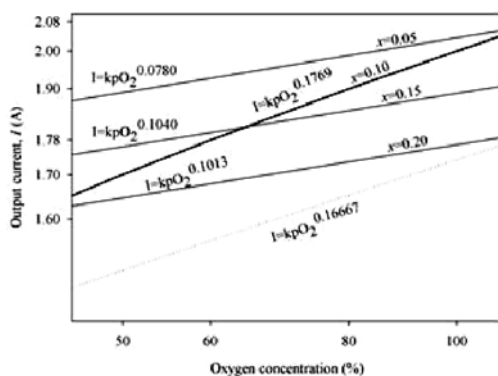
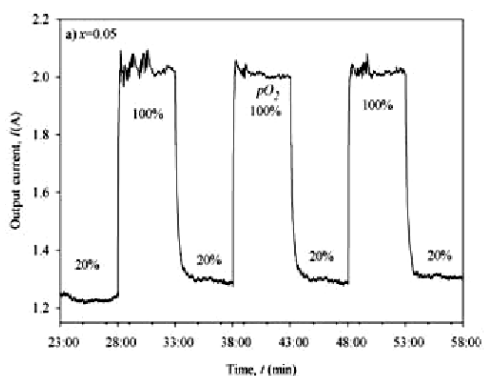
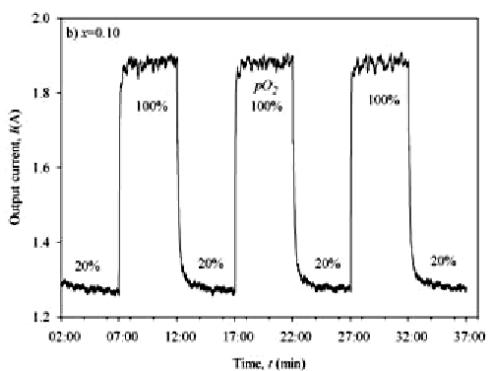


Figure 4. Graph of log output current versus log pO_2 at high oxygen concentration. Thick line show the closest value to the ideal case of conductivity to $pO_2^{1/6}$ which is indicated by dotted line.

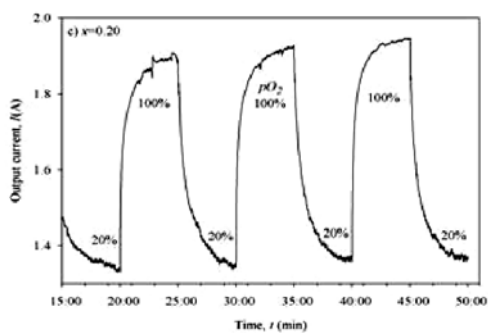
Figure 4 shows the graph of log of output current versus log of pO_2 . The dotted line shows the case where σ is proportional to $pO_2^{1/6}$ as expressed by equation (2). From the gradients of the plots, it can be seen that the rod with $x = 0.1$ has the closest value to $1/6$ indicating that it closely abide to the conductivity expressed by the equation.



(a)



(b)



(c)

Figure 5. Repeatability of output current between 20% $p\text{O}_2$ and 100% $p\text{O}_2$ and vice versa with interval of 5 minutes at temperatures above 75°C .

Figure 5 shows repeatability of output current between 20% pO_2 and 100% pO_2 at temperatures above 750°C. Since the absorption rate depends on temperature, T and can be described using the Arrhenius law behaviour for temperature dependence respond time,

$$t_{res} = t_o \exp\left(\frac{E_a}{k_B T}\right), \quad (3)$$

where t_{res} is the time taken for the output current to reach saturated level, t_o is a constant independent of temperature, T , E_a is the activation energy of ionic migration and k_B is the Boltzmann constant [6]. From Figure 5, t_{res} was longer as the amount of x increases especially for rods with $x > 0.1$. This implies that, as the amount of Pr substituted at Eu-site increases, the absorption time and desorption time becomes longer.

In terms of stability after the output current reached saturation level, the $x = 0.1$ rod showed more stability than the other rods. This could be due to its hot-spot temperature reaching the optimum level for the output current to be stabilized as reported by previous studies where stability of output current is temperature dependent [4, 6, 7].

The activation energy, E_a as shown in Table 1, increases as the amount of Pr was increased. This may be due to the involvement of oxygen from other locations in the structure which have stronger bond compared to oxygen in the Cu-O chains. Thus the absorption and desorption processes of oxygen into the structure required a lot more energy. As a result, E_a , increases with increasing Pr substitution.

4. Conclusions

The I - V characteristics and oxygen sensing behaviour of $\text{Eu}_{1-x}\text{Pr}_x\text{Ba}_2\text{Cu}_3\text{O}_{7-\delta}$ ceramic rods were studied. XRD analysis showed that Pr doping reduces the orthorhombicity while still preserving orthorhombic structure. The decrease in unit cell volume, Ω and c -lattice

parameter with increasing Pr doping indicated possible Pr substitution at Eu-site of $\text{Eu}_{1-x}\text{Pr}_x\text{Ba}_2\text{Cu}_3\text{O}_{7-\delta}$. All rods showed output current, after the formation of hot-spot, depends on oxygen concentration. Sensitivity for all rods increased for oxygen concentration 20% to 50% (lower pO_2) but reduces as the oxygen concentration increased from 60% to 100% (higher pO_2). Interestingly, doping prevented the sensitivity from dropping to almost zero as previously reported for $\text{Eu}(\text{Ba}_{1-x}\text{Pr}_x)_2\text{Cu}_3\text{O}_{7-\delta}$ rods due to existence of Cu-O chains in the orthorhombic structure. The increase in activation energy, E_a with Pr doping indicated more energy was required for the absorption and desorption of oxygen to take place as the process may also involve oxygen from other locations in the structure which has stronger bond compared to oxygen in the Cu-O chains. Among all the rods, the dependency of the output current on pO_2 for the rod with $x = 0.10$ has the closest value to the ideal case (σ proportional to $pO_2^{1/6}$), indicating that the conductivity closely obeys the expression of equation (2). The doping of $x = 0.10$ resulted in better oxygen absorption response time, t_{res} and better output current stability compared to other rods.

Acknowledgment

This research has been supported by the Malaysian Ministry of Higher Education under Fundamental Research Grant Scheme no.: UiTM-600-RMI/FRGS 5/3/(60/2013).

References

- [1] M. Takata, Y. Noguchi, Y. Kurihara, T. Okamoto and B. Huybrechts, Bull. Mater. Sci. 22 (1999), 593.
- [2] T. Okamoto and M. Takata, Ceramic International 30 (2004), 1569-1574.

- [3] S. A. Yaacob, A. K. Yahya, M. I. M. Yusof and R. Hasham, Effect of divalent ion substitution on oxygen sensing properties of hot-spot based $\text{Eu}_{1-x}\text{Ca}_x\text{Ba}_2\text{Cu}_3\text{O}_{7-\delta}$ and $\text{Eu}_{1-y}\text{Mg}_y\text{Ba}_2\text{Cu}_3\text{O}_{7-\delta}$ ceramics, *Ceramics International* 38 (2012), 6311-6319.
- [4] M. I. Adzam, M. I. M. Yusof and A. K. Yahya, Influence of Pr^{3+} substitution at Ba-site of $\text{Eu}(\text{Ba}_{1-x}\text{Pr}_x)_2\text{Cu}_3\text{O}_{7-\delta}$ ceramic rods with hot-spot on oxygen sensing properties, *Ceramics International* 39 (2013), S743-S746.
- [5] L. H. Idrus, T. Okamoto and A. K. Yahya, Effect of ionic size on oxygen sensing properties of Sr-substituted Ho123 ceramic rods utilizing hot-spot phenomena, *Materials Research Innovations* 15 (2011), 144-147.
- [6] M. Hassan and A. K. Yahya, Influence of hot-spot temperature on oxygen sensing response behaviour of Er123 ceramic rods with hot-spot, *J. Alloys Compd.* 499 (2010), 206-211.
- [7] S. A. Yaacob, A. K. Yahya, M. Hassan and R. Hasham, Influence of intrinsic hole concentration on oxygen sensing properties of hot-spot based $\text{Eu}_{1-x}\text{Ca}_x\text{Ba}_2\text{Cu}_3\text{O}_{7-\delta}$ ceramics, *AIP Conf. Proc.* 1250, pp. 313-316, doi:<http://dx.doi.org/10.1063/1.3469666>.
- [8] H. Sunatori and T. Okamoto and M. Takata, *J. Ceram. Soc. Japan* 111 (2003), 217.
- [9] Y. Kurihara, Y. Noguchi and M. Takata, *Key Eng. Mater.* 157 (1999), 127.
- [10] Y. Kurihara, T. Okamoto, B. Huybrechts and M. Takata, *J. Mater. Res.* 11 (1996), 549.
- [11] L. Shi, Y. Huang, Y. Jia, X. Liu, G. Zhou and Y. Zhang, Study on the crystal and electronic structure of $\text{Y}_{1-x}\text{Pr}_x\text{Ba}_2\text{Cu}_3\text{O}_{7-\delta}$ ceramics, *J. Phys. Condens. Matter* 10 (1998), 7015-7024.
- [12] E. Klencsar, Z. Kuzmann, A. Homonnay, K. Vertes, J. Vad, T. Bankuti, M. Racz and I. Bodog, Kotsis The effect of Pr substituted in $\text{Eu}_{1-x}\text{Pr}_x\text{Ba}_2\text{Cu}_3\text{O}_{7-\delta}$ and $\text{EuBa}_{2-x}\text{Pr}_x\text{Cu}_3\text{O}_{7-\delta}$ perovskites, *Physica C* 304 (1998), 124-132.
- [13] S. J. Gurman, J. C. Amiss, M. Khaled, N. L. Saini and K. B. Garg, X-ray absorption study of the $(\text{Y}_{1-x}\text{Pr}_x)\text{Ba}_2\text{Cu}_3\text{O}_{7-\delta}$ system, *J. Phys. Condens. Matter* 11 (1999), 1847-1859.
- [14] E. B. Mitberg, M. V. Patrakeev, I. A. Leonidov, A. A. Lakhtin, V. L. Kozhevnikov and K. R. Poeppelmeier, *J. Alloys Compd.* 274 (1998), 98-102.

- [15] G. Flor, G. Chiodelli, G. Spinolo and P. Ghigna, *Physica C: Supercond.* 316 (1999), 13-20.
- [16] G. Chiodelli, I. Wenneker, P. Ghigna, G. Spinolo, G. Flor, M. Ferretti and E. Magnone, *Physica C: Supercond.* 308 (1998), 257-263.
- [17] M. Akhavan, The question of Pr in HTSC, *Physica B* 321 (2002), 265-282.
- [18] Youwen Xu, M. J. Kramer, K. W. Dennis, H. Wub, A. O'Connor, R. W. McCallum, S. K. Malik and W. B. Yelon, Substitution for Ba by Pr, La, and Eu in $\text{Eu}(\text{Ba}_{1-x}\text{Pr}_x)_2\text{Cu}_3\text{O}_{7-\delta}$ solid solutions, *Physica C* 333 (2000), 195-206.